A&A manuscript no.
(will be inserted by hand later)

Your thesaurus codes are:
02.12.1, 08.01.1, 08.01.2, 08.01.3, 10.15.2 Pleiades

ASTRONOMY
AND
ASTROPHYSICS
2.12.1996

Modeling Li I and K I sensitivity to Pleiades activity

R. Stuik[1,2], J.H.M.J. Bruls[2], and R.J. Rutten[1]

[1] Sterrekundig Instituut, Postbus 80000, NL–3508 TA Utrecht, The Netherlands
[2] Instituto de Astrofísica de Canarias, C./ Via Láctea s/n, E–38200 La Laguna, Tenerife, Spain

Received date; accepted date

Abstract. We compare schematic modeling of spots and plage on the surface of cool dwarfs with Pleiades data to assess effects of magnetic activity on the strengths of the Li I and K I resonance lines in Pleiades spectra. Comprehensive Li I and K I NLTE line formation computation is combined with comparatively well-established empirical solar spot and plage stratifications for solar-like stars. For other stars, we use theoretical constructs to model spots and plage that portray recipes commonly applied in stellar activity analyses. We find that — up to B–$V \approx 1.1$ — neither the Li I 670.8 nm nor the K I 769.9 nm line is sensitive to the presence of a chromosphere, in contrast to what is often supposed. Instead, both lines respond to the effects of activity on the stratification in the deep photosphere. They do so in similar fashion, making the K I line a valid proxy to study Li I line formation without spread from abundance variations. The computed effects of activity on line strength are opposite between plage and spots, differ noticeably between the empirical and theoretical solar-like stratifications, and considerably affect stellar broad-band colors. Our results indicate that one can neither easily establish, nor easily exclude, magnetic activity as major provider of K I line strength variation in the Pleiades. Since Li I line formation follows K I line formation closely, the same holds for Li I and the apparent lithium abundance.

Key words: Line: formation – Stars: abundances – Stars: activity – Stars: atmospheres – Pleiades

1. Introduction

This paper is a sequel to Carlsson et al. (1994) by taking up the point made in its last sentence. It stated that the large variation in K I 769.9 nm line strength shown for Pleiades stars in Fig. 4 of Soderblom et al. (1993a) implies that the similar spread in Li I 670.8 nm line strength may not be attributed simply to differences in lithium abundance without detailed line formation evaluation. We elaborate on this point here with numerical modeling of the sensitivity of both K I 769.9 nm and Li I 670.8 nm to cool-star magnetic activity, and so add fuel to the many ongoing debates on stellar lithium content. These are reviewed by e.g., Boesgaard (1990a 1990b); Michaud & Charbonneau (1991); Rebolo (1990, 1991); Spite (1990, 1991, 1995); Soderblom (1991, 1995, 1996); Strom (1994); Thorburn (1995), and in the introductory section of Carlsson et al. (1994).

The context of our study is defined by Figs. 2c and 4 of Soderblom et al. (1993a). Their paper is the major Pleiades analysis in recent years and is the principal reference addressed here (but see also Soderblom et al. 1993b, 1993c; Soderblom 1995; Russell 1996). Similar displays from the same data are shown in our Fig. 1. Plotted against unreddened B–V, the observed strength of Li I 670.8 nm in the upper panel shows a well-known overall pattern (e.g., Gray 1992, p. 323) in which the initial rise with B–V is due to the increase of the population fraction of the neutral lithium stage, whereas the average decline for B–$V > 0.8$ portrays increasing lithium depletion. Its lower envelope does not reach as far down as in corresponding plots for older clusters such as the Hyades and Praesepe (cf. Fig. 9 of Soderblom et al. 1993a). This fact indicates that the cooler Pleiades are still being depleted in the classical convective Li(p,α)He burning originally proposed by Greenstein & Richardson (1951) and subsequently established by Bodenheimer (1965), Iben (1965, 1966, 1967), Herbig (1965) and Wallerstein et al. (1965).

In addition, the upper panel of Fig. 1 shows large upward spread above the lower envelope, especially for B–$V > 0.8$. It is much larger for the Pleiades than for the older clusters, of order two dex in corresponding lithium abundance for B–$V > 0.8$. It was first called to attention by Duncan & Jones (1983), was studied by Balachandran et al. (1988), Soderblom et al. (1990, 1993a, 1993b), Soderblom (1991), Stauffer et al. (1993), Thorburn et al. (1993) and Russell (1996). It was reviewed most recently by Soderblom (1995, 1996). This spread is the topic of this paper.

Send offprint requests to: R.J. Rutten

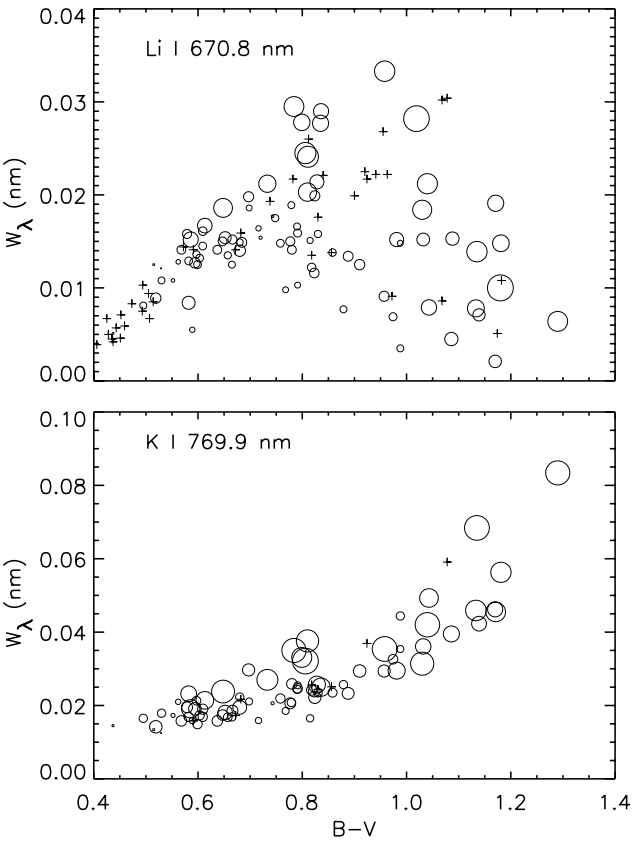

Fig. 1. Equivalent widths of Li I 670.8 nm (*upper panel*) and K I 769.9 nm (*lower panel*) in Pleiades spectra against B–V color. The latter is "unreddened", i.e., corrected for interstellar extinction. The circles mark Pleiades members for which chromospheric emission was estimated from the fill-in of the Ca II 854.2 nm line core, increasing size denoting larger magnetic activity. The upper panel shows the effect of lithium depletion for B–$V > 0.8$. Both lines show correlation between line strength and chromospheric activity. Data from Soderblom et al. (1993a)

In lithium astronomy, variations in Li I 670.8 nm line strength are habitually taken to measure differences in lithium abundance. Doing so for the Pleiades, while assuming that these cluster members share the same age and initial lithium concentration, implies that the spread in the upper panel of Fig. 1 marks differences in lithium depletion that should vanish by the time the Pleiades become as old as the Hyades. Presumably, these differences are primarily set by the stellar rotation rate and its history, with lower depletion rate for larger rotation as proposed by e.g., Pinsonneault et al. (1989, 1990). Indeed, the spread in the upper panel of Fig. 1 possesses an apparent correlation between Li I 670.8 nm line strength and rotation velocity that is most outspoken for the lithium-rich "ultrafast rotators" (Fig. 2b of Soderblom et al. 1993a). In a nutshell, such attribution of the Li I Pleiades spread to rotationally created abundance differences forms the main conclusion of Soderblom et al. (1993a). They rejected the earlier hypothesis of Duncan & Jones (1983) and Butler et al. (1987) that the spread marks considerable inequality in Pleiades birth dates.

Before reaching their conclusion, Soderblom et al. (1993a) examined and rejected other possible causes of Li I 670.8 nm line strength variations. Stellar activity is the most obvious one. In general, it increases with stellar rotation. Indeed, Favata et al. (1995) have in the meantime demonstrated Pleiades correlations between X-ray emission, Li I line strength and rotation rate (see also Stauffer et al. 1994). The open circles in Fig. 1 mark Pleiades for which also the Ca II 854.2 nm line was measured. The symbol size increases with Ca II line-center intensity and should therefore encode the degree of activity since chromospheric emission fills in the line. There is a rough correlation, most significant in the left half of the upper panel, in the sense that the larger symbols (weaker Ca II line) prefer to lie at relatively large Li I line strength. The issue addressed here is whether this correlation displays intrinsic lithium abundance differences that are controlled by difference in stellar rotation rate and vary along with stellar activity without a direct causal relationship, or whether the stellar activity itself causes Li I line strength variations at given lithium content by modifying the atmospheric stratification locally and so affecting the surface-integrated spectrum. In the latter case, the next question is to what extent such non-abundance line formation variations may explain the observed spread.

Obviously, the issue of lithium abundance versus activity is not a new one; we refer the reader to the many reviews cited above and to our extensive introduction in Carlsson et al. (1994). Hultqvist (1974, 1977) studied the production of lithium by spallation reactions in solar flares, as actually measured later by Murphy et al. (1990). Duncan (1981) was the first to search for relations between Li I and Ca II K line strengths, finding less strong correlations between these two measures for field stars than expected from the fact that both diminish statistically with stellar age. Giampapa (1984) observed that Li I 670.8 nm weakens in solar plage and strengthens greatly in umbrae, and suggested that these changes may affect the observed line strength from stars with large spot and/or plage coverage. Rotational modulation of the line strength has not been found (Boesgaard 1990a), not even for the heavily spotted RS Cvn stars (Pallavicini et al. 1987; Pallavicini et al. 1992; Randich et al. 1992; Randich et al. 1993; Pallavicini et al. 1993), but the four stars monitored by the latter authors did display considerable Li I 670.8 nm profile variations at constant equivalent width.

Soderblom et al. (1993a) used the K I 769.9 nm resonance line as an observational check on this issue. It is similar in formation to Li I 670.8 nm. Since the stel-

lar potassium content is not suspected of lithium-like depletion variations between Pleiades, the observed K I 769.9 nm spread may delineate the non-abundance part of the observed Li I 670.8 nm spread. The result is shown in Fig. 4 of Soderblom et al. (1993a), and is replotted here in the lower panel of Fig. 1. The K I 769.9 nm line strength does indeed not share the turnover and decrease for B–$V > 0.8$ that marks lithium depletion in the upper panel. In that part of the diagram, the upward K I spread is also markedly smaller. However, for B–$V < 0.8$ the K I spread appears rather similar to the Li I spread, again with apparent correlation between line strength and chromospheric Ca II 854.2 nm fill-in.

Soderblom et al. (1993a) state that the non-abundance spread indicated by K I in the lower panel of Fig. 1 is appreciably smaller than the observed Li I spread in the upper panel. They argue that chromospheres cannot explain the latter since a chromospheric temperature rise should depopulate the neutral lithium stage and so weaken the Li I 670.8 nm line rather than strengthen it, whereas it shouldn't affect the deeper-formed Li I 610.4 nm line which is observed to strengthen together with Li I 670.8 nm. They then discussed the influence of star spots, showing from simple LTE modeling with variation in spot temperature and stellar spottedness that these may explain any observed Li I 670.8 nm scatter — but only in unlikely fashion, requiring large filling factors that should also upset the photometric properties of the stars.

In the present study we re-address this issue of Li I sensitivity to Pleiades activity. It is triggered by the K I spread for B–$V < 0.8$ in the lower panel of Fig. 1, which seems about as large as the Li I spread in the upper panel. This spread indicates that otherwise comparable solar-type Pleiades differ sufficiently in atmospheric stratification to produce markedly different alkali resonance lines. The K I spread must be clarified in detail before one may safely ignore it in order to attribute the observed Li I spread to intrinsic abundance variations. We therefore concentrate in this paper on K I line formation along with Li I line formation. Compared with Soderblom et al. (1993a), we add sophistication by combining proven NLTE modeling techniques (Carlsson et al. 1994) for both Li I and K I with more detailed models for active-atmosphere stratifications, not only of starspots but also for plage, and by using elaborate empirical modeling of sunspots and solar plage as a guide. However, our study remains a schematic feasibility analysis. Our aim is to estimate the bandwidth of uncertainty that stellar activity brings to discussions of Pleiades lithium content.

The organization of the paper is as follows. In Sect. 2 we present our methods and models. Our results are split between the use of established empirical models for sunspot umbrae and solar plage fluxtubes (Sect. 3.1), and more naive modeling of these basic elements of activity for other dwarf stars (Sect. 3.2). We find inconsistency between the two approaches, especially for plage, with repercussions on B–V to $T_{\rm eff}$ conversion (Sect. 4). The main conclusion of this paper is that stellar activity modeling is yet far too model-dependent to derive quantitative corrections (Sect. 5). Only comprehensive, self-consistent reproduction of a complete set of diagnostics may quantify to what extent lithium lines in Pleiades spectra betray surface structure variations rather than abundance variations.

2. Method and models

Method. We use the program MULTI by Carlsson (1986) which implements the operator perturbation technique of Scharmer & Carlsson (1985) to compute NLTE emergent flux profiles of Li I 670.8 nm, Li I 610.4 nm and K I 769.9 nm for a grid of solar and stellar atmospheres with different amounts of magnetic activity. We characterize the latter by the presence of spots and plage, using existing empirical models of sunspot umbrae and solar facular fluxtubes to model these structures for solar-type Pleiades. We also use schematic constructs for dwarfs of other spectral type that apply the ad-hoc recipes often used in stellar activity modeling. These models are detailed below.

The magnetic-structure line profiles that result from these models are mixed with standard radiative-equilibrium (RE) profiles in a simple procedure. It consists of computing the equivalent width $W_{\rm RE}$ of the emergent flux profile $F_{\rm RE}(\nu)$ of a given line for a given RE model and computing, separately and similarly in plane-parallel fashion, the equivalent widths $W_{\rm s}$ and $W_{\rm p}$ of the emergent flux profiles $F_{\rm s}(\nu)$ and $F_{\rm p}(\nu)$ for the corresponding spot umbra and plage fluxtube models. We then assume that the flux at the surface of a star that is covered by umbrae and fluxtubes with area filling factors $\alpha_{\rm s}$ and $\alpha_{\rm p}$, respectively, is given by the area-weighted summation

$$F(\nu) = (1 - \alpha_{\rm s} - \alpha_{\rm p})F_{\rm RE} + \alpha_{\rm s}F_{\rm s}(\nu) + \alpha_{\rm p}F_{\rm p}(\nu), \qquad (1)$$

so that the spatially-averaged emergent flux profile has equivalent width

$$W_\lambda = \frac{(1 - \alpha_{\rm s} - \alpha_{\rm p})F^c_{\rm RE}W_{\rm RE} + \alpha_{\rm s}F^c_{\rm s}W_{\rm s} + \alpha_{\rm p}F^c_{\rm p}W_{\rm p}}{(1 - \alpha_{\rm s} - \alpha_{\rm p})F^c_{\rm RE} + \alpha_{\rm s}F^c_{\rm s} + \alpha_{\rm p}F^c_{\rm p}} \qquad (2)$$

where the index c denotes background continuum flux. The final assumption is to equate this surface-flux equivalent width to the equivalent width of the irradiance profile measured at Earth. This procedure assumes homogeneous distributions of the magnetic elements over the stellar surface, and ignores second-order geometry effects as Wilson depressions, departures from one-dimensional radiative transfer (slanted lines of sight cutting through the magnetic elements) and profile variations due to rotation that are not described by simple convolution (cf. Bruning 1981, Rutten & van der Zalm 1984, Gray 1992). Our recipe is simpler than the more elaborate spot model used by Torres & Mello (1973), Vogt (1981) and Bouvier et al. (1993), but it suffices for the present application. It

is comparable to the recipes applied by Giampapa (1984), Robinson et al. (1986) and Pallavicini et al. (1993).

Model atoms. Our lithium model atom is the one constructed by Carlsson et al. (1994). It has 21 levels and 70 lines; the $2p$ level has explicit fine-structure splitting in order to separate the two components of the $2p$–$2s$ resonance doublet. The lithium abundance was set to $A_{\rm Li} = 3.0$ on the standard scale where $A_{\rm Li} \equiv \log(n_{\rm Li}/n_{\rm H}) + 12$. This value was taken as characteristic for the Pleiades (cf. Fig. 2 of Boesgaard 1991) and is used in all modeling below.

The potassium model atom comes from Bruls et al. (1992). It is the largest "confection atom" shown in their Fig. 20, contains 13 levels and 17 lines, and was also employed by Bruls & Rutten (1992). The potassium abundance is set to $A_{\rm K} = 5.13$ after Anders & Grevesse (1989).

A difference with the Li I modeling of Carlsson et al. (1994) and the K I modeling of Bruls et al. (1992) is that we do not account for the ultraviolet line haze in the photoionization rate evaluations, for want of a practical and reliable formalism for NLTE line blanketing (called "the last problem of classical stellar atmospheres" by Hubeny & Lanz 1995). Since we do not aim to reproduce observed line profiles in detail, we prefer not to make ad-hoc choices regarding line-haze source functions. Note, however, that the Uppsala model atmospheres discussed below do include LTE line blanketing.

Test calculations were also performed with MULTI's benchmark six-level calcium atom in order to evaluate the chromospheric emission in the Ca II 854.2 nm line. These are not displayed here, but confirm that the chromospheric temperature rises in our solar spot and plage models produce fill-in of this line.

Solar models. The upper panel of Fig. 2 displays our solar models. The non-magnetic solar surface is represented by the $T_{\rm eff} = 5750$ radiative equilibrium model (solid curve marked RE) from the Uppsala sequence discussed below. By definition it has no chromospheric temperature rise. The photospheric part is close to current empirical quiet-Sun models (see comparison in Fig. 2 of Carlsson et al. 1992).

The sunspot model is the umbral model of Maltby et al. (1986), with corrections of typing errors that affect the electron densities. This model has been criticized by Caccin et al. (1993), leading Severino et al. (1994) to constrain the umbral temperature gradient in the upper photosphere from the inner wings of the Na I D lines. They found that the flat part seen in Fig. 2 should be replaced with an outward decline similar to a non-grey radiative equilibrium gradient (their Fig. 4). However, Figs. 3–4 below show that neither the Li I 670.8 nm nor the K I 769.9 nm equivalent width is sensitive to this part of the temperature stratification.

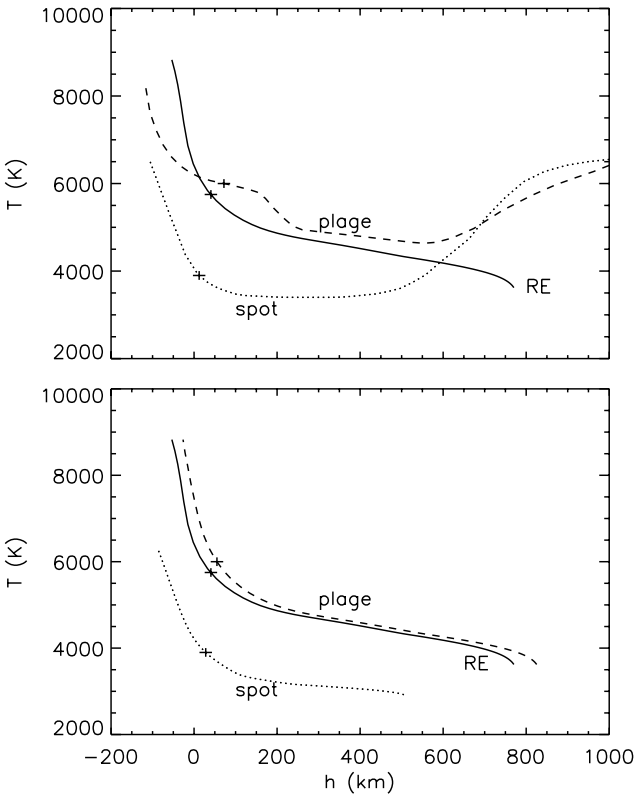

Fig. 2. Temperature stratifications. Each model is shown on its own height scale, with $h = 0$ km at $\tau_{500} = 1$. The crosses mark the effective temperature per model. *Upper panel:* solar models. The radiative-equilibrium stratification (RE) is the $T_{\rm eff} = 5750$ model from the Uppsala grid. The sunspot umbra and plage fluxtube stratifications are empirical models from the literature. *Lower panel:* stellar modeling for $T_{\rm eff} = 5750$ K. The RE model is the same as in the upper panel. The spot umbra is described by an Uppsala RE model with lower (65%) effective temperature. The stratification of the plage fluxtube is derived from the RE model by requiring thin-tube magnetostatic equilibrium with the same temperature within and outside the fluxtube

The solar plage model in Fig. 2 is the PC1 fluxtube model of Bruls & Solanki (1993). It combines the PLA fluxtube model of Solanki & Brigljevic (1992) with the chromospheric temperature rise of the standard quiet-Sun model of Maltby et al. (1986). The latter is not sensed by the Li I and K I resonance lines. A more important feature of this model is the hump in deeper layers. It consists of a fairly flat temperature gradient just above $h = 0$ (corresponding to optical depth unity in the continuum at $\lambda = 500$ nm) and a steep drop just below $h = 200$ km. This hump is derived from detailed Stokes–V modeling of numerous Fe I lines (cf. Solanki 1986) and was confirmed by the direct inversion of Stokes spectra by Keller et al. (1990).

The "microturbulent" broadening parameter was set to 1 km s^{-1}, except for the sunspot model for which the

height-dependent tabulation of Maltby et al. (1986) was used.

Stellar modeling. For other stars than the Sun there exist no detailed magnetic-element models comparable to the well-established empirical sunspot and plage models displayed above. We therefore apply traditional recipes to construct stellar spot and plage models in simple manner. In order to enable comparison with the empirical solar modeling, we also construct such theoretical models for solar-like Pleiades.

Our starting point is a sequence of standard radiative-equilibrium models computed with the Uppsala MARCS code of Gustafsson et al. (1975) and kindly made available by Mats Carlsson (Oslo). These are state-of-the art plane-parallel, line-blanketed, flux-constant LTE atmospheres. Although they are called "radiative-equilibrium" (RE) here, they do include convective energy transport in their deepest layers using the mixing-length approximation. The line blanketing is treated with opacity distribution functions and LTE source functions. The sequence is for dwarf stars with solar surface gravity ($\log g = 4.44$), solar metallicity ([Fe/H] $= 0.0$) and 1 km s^{-1} microturbulence. It covers the range $T_{\rm eff} = 4000 - 7000$ K in 250 K steps. Figure 2 shows the $T_{\rm eff} = 5750$ Uppsala model in both panels (RE).

For starspot modeling we simply take Uppsala models with lower effective temperature than the stellar model under consideration. Denoting the latter by $T^*_{\rm eff}$, we interpolate new models from the range of RE models for $T_{\rm eff} = 0.65\,T^*_{\rm eff}$ and $T_{\rm eff} = 0.85\,T^*_{\rm eff}$. Reduction to 65% corresponds to the solar case in the upper panel of Fig. 2. It produces a spot model (lower panel) that does not differ much from the empirical model in the upper panel. It actually conforms to the modification of the latter proposed by Severino et al. (1994). For cooler $T^*_{\rm eff}$ there are no models available in the Uppsala sequence with sufficiently low temperature to permit such 0.65 reduction; the 0.85 factor serves to obtain spot models for these. This factor corresponds with empirical determinations of cool-star spot temperatures (cf. Neff et al. 1995, O'Neil et al. 1996), as does the overall 0.65–0.85 range (cf. Byrne 1992). The range also contains the values chosen by Giampapa (1984), Robinson et al. (1986) and Pallavicini et al. (1993).

In order to obtain stellar plage models, we have computed stratifications in the "thin-tube" approximation (e.g., Defouw 1976, Schüssler 1986, Bruls & Solanki 1993) in which all radial derivatives of state parameters within the tube are set to zero. In addition, we assume temperature equality at each height between the fluxtube inside and outside (this is, for optically thin fluxtubes, achieved by lateral radiative exchange), pressure equilibrium between inside and outside, hydrostatic equilibrium vertically inside the tube (as there is outside), and magnetic field strengths at the base of the fluxtube that diminish from $B = 2000$ Gauss for $T_{\rm eff} = 4000$ K to $B = 1000$ Gauss at $T_{\rm eff} = 7000$ K to follow the decline of the outside gas pressure at base height. The resulting fluxtube atmospheres, of which the $T_{\rm eff} = 5750$ example is shown in the lower panel of Fig. 2, duplicate the RE models at smaller densities and with different density–height relations (the height scales of Figs. 2–4 are shifted per model over the corresponding Wilson depression). Their effective temperatures are about 200 K higher than for the surrounding RE atmosphere over the whole Uppsala sequence. In contrast to the starspot and sunspot models, Fig. 2 shows large disparity between the stellar plage model in the lower panel and the empirical solar fluxtube model in the upper panel. The stellar model has no hump above the $\tau_{500} = 1$ height and has no cross-over with the RE model in deeper layers. These differences produce large effects in our results below.

Color and effective temperature. By replacing parts of the stellar surface with cooler (spots) and hotter (plage) material, we change the apparent color and effective temperature of the star. These changes differ in nature, since effective temperature measures the integrated flux while colors measure the flux distribution slope. The change in effective temperature follows for any combination of filling factors from Eq. 1, but the corresponding color change must be found numerically. We have evaluated the apparent color B–V by integration over the B and V passbands as tabulated by Allen (1976), neglecting spectral lines. This was done, per filling factor combination, for all results presented in Figs. 7–11 below.

3. Results

3.1. Solar models

NLTE line formation. Figures 3 and 4 display the formation of Li I 670.8 nm and K I 769.9 nm, respectively, for the three solar models. The model temperatures are again shown in the middle panel, together with the line excitation temperature $T_{\rm exc}$ which displays line source function behavior expressed as temperature. This format makes the source functions of the two lines directly comparable by eliminating Planck function variations with wavelength. The top panel shows NLTE departure population coefficients for the upper and lower levels in the abundance-normalized convention of Wijbenga & Zwaan (1972; cf. Sect. 4.3.6 of Rutten 1996). The bottom panels show the resulting flux profiles.

The NLTE behavior seen in the upper panels poses no surprises. The alkali NLTE mechanisms have been analyzed in detail by Bruls et al. (1992) and are summarized by Carlsson et al. (1994); for tutorial background see Rutten (1996). The Li I $2s$ ground state does not show a bulge for the RE model due to photon suction as it does in the comparable Fig. 4 of Carlsson et al. (1994) because our lithium abundance is half the value used there

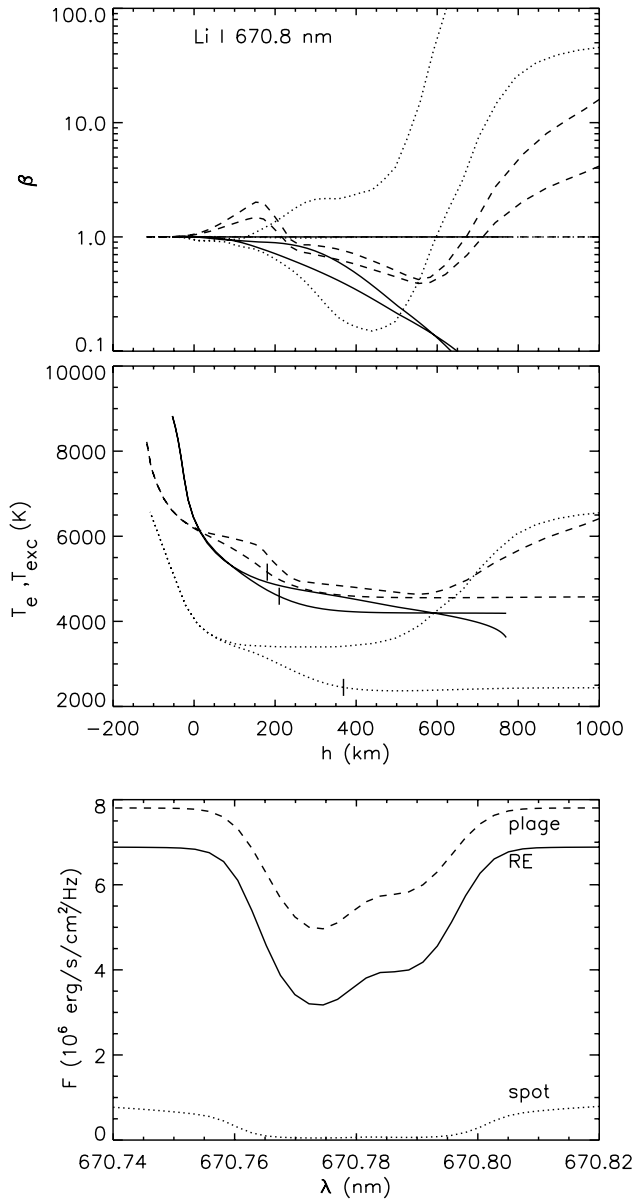

Fig. 3. Formation of the Li I 670.8 nm resonance doublet for the three solar models. Curve coding as in Fig. 2. *Top panel:* NLTE departure coefficients $\beta = n_i/n_i^{\rm LTE}$ for the $2s$ Li I ground state (upper curve for each pair) and the $2p$ upper levels of Li I 670.8 nm (lower curves). *Middle panel:* model temperatures $T_{\rm e}$ as in Fig. 2 (upper curve of each pair) plus line source functions in the form of excitation temperatures $T_{\rm exc}$. The ticks mark locations with total optical depth unity at line center. *Bottom panel:* emergent flux profiles

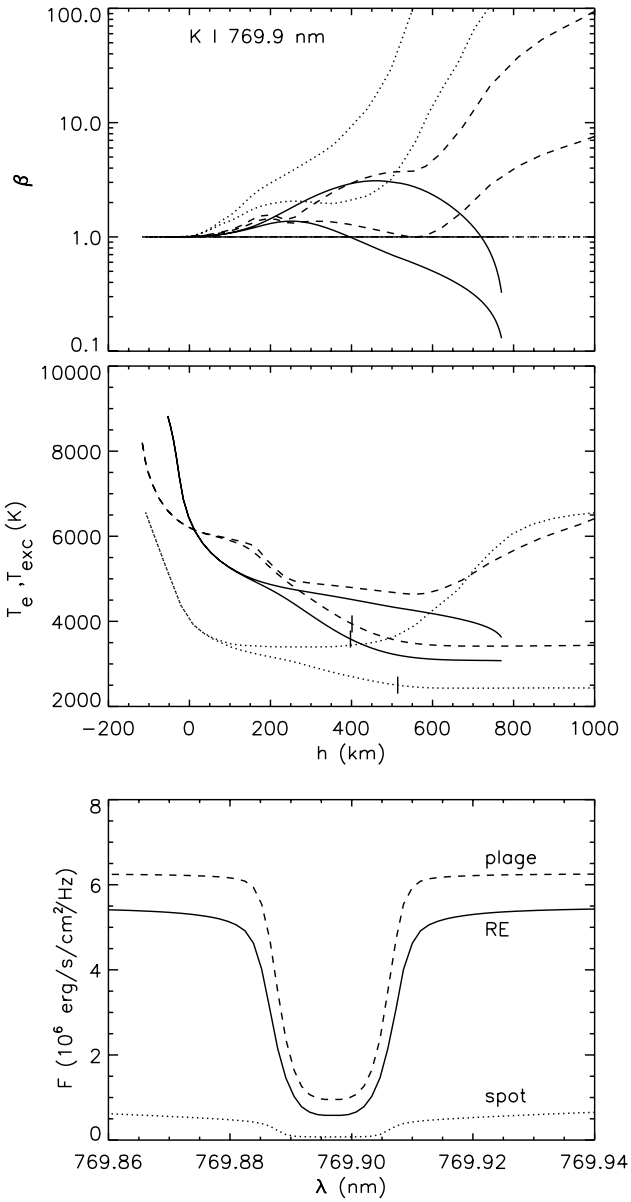

Fig. 4. Formation of the K I 769.9 nm resonance line for the three solar models. Panel layout and curve coding as in Fig. 3. The departure coefficients in the upper panel are for the $4s$ K I ground state (upper curve of each pair) and the $4p$ upper level of K I 769.9 nm

and because there is larger overionization in our modeling since we do not account for ultraviolet line blocking. The plage atmosphere provides less ultraviolet radiation and produces overrecombination. The cool spot atmosphere contains much more neutral lithium (outward shift of the $\tau = 1$ tick), enough to make the Li I 670.8 nm doublet suffer markedly from NLTE resonance scattering (evident as large split between the dotted curves in both the upper and middle panels). The large effective photon losses drive a suction replenishment flow that doubles the neutral-stage population above $h = 200$ km. Scattering is much less important in the RE and plage atmospheres.

The K I results in Fig. 4 show similar behavior at larger line opacity and smaller ground-state photoionization. Scattering affects K I 769.9 nm in all three atmospheres and causes neutral-stage overpopulation through photon suction from the ion population which reaches an

order of magnitude for the sunspot. For this atmosphere, the $\tau = 1$ tick lies at the onset of the chromospheric temperature rise, but the latter is not sensed by the line source function since it is fully dominated by the radiation field at that height.

Emergent profiles. The bottom panels of Figs. 3–4 show that the solar plage atmosphere produces higher continuum flux than the RE atmosphere. The two temperature stratifications are nearly equal at their respective $\tau_{500} = 1$ locations, corresponding to the absence of contrast between solar plage and its surroundings when observed at disk center in the $\lambda = 500$ continuum. The emergent flux spectrum at the longer alkali-line wavelengths shows larger contrast because the characteristic $\tau_\lambda = 2/3$ formation height lies further out than $\tau_{500} = 1$ and the hump of the plage model is sensed by the outward tail of the contribution function. The effective temperature of the plage model is also higher than the RE case (crosses in Fig. 2).

The Li I 670.8 nm feature in Figs. 3–4 has, by virtue of being a doublet, only slightly smaller equivalent width than the K I 769.9 nm line for all three models. The equivalent widths increase from plage to RE to sunspot; the sunspot profiles combine low continuum flux with very large equivalent width (they possess extended wings that are cut off by the figure frame; the sunspot continuum flux is $F = 1.02 \times 10^6$ erg/s/cm^2/Hz for both lines).

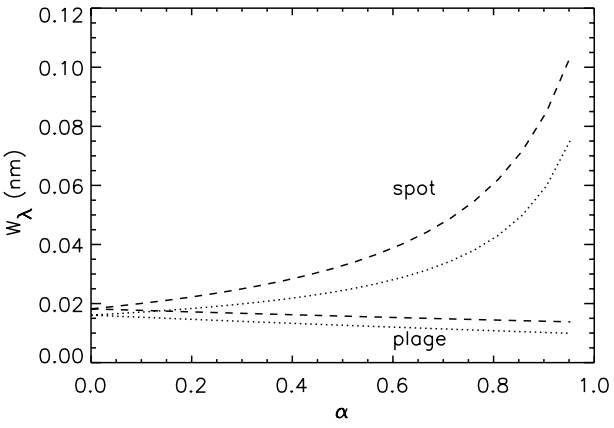

Fig. 5. Computed equivalent widths of Li I 670.8 nm (*dotted*) and K I 769.9 nm (*dashed*) against filling factor α when combining the $T_{\rm eff} = 5750$ RE model with sunspot umbrae and solar facular fluxtubes, respectively. The Li I and K I resonance features have similar sensitivity to magnetic activity

Sensitivity to magnetic area. Figure 5 displays the dependence of Li I 670.8 nm and K I 769.9 nm irradiance line strength on the filling factors $\alpha_{\rm s}$ and $\alpha_{\rm p}$ for the solar models. Obviously, values $\alpha = 1$ are unrealistic; a Sun covered

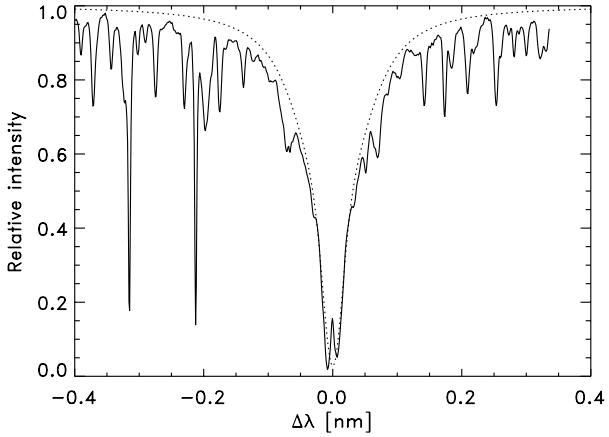

Fig. 6. The K I 769.9 nm line in a sunspot umbra. The tracing is from high-resolution FTS data obtained by O. Engvold and J.W. Brault at Kitt Peak in 1981. The dotted curve is a simple fit. It has $W_\lambda = 0.107$ nm

100% by umbrae or facular fluxtubes is no longer a solar-type star. Even within actual solar plage, the fluxtubes represented by the plage model have typical filling factors of only $\alpha_{\rm p} = 0.1 - 0.3$, perhaps up to 0.5 over small areas (e.g., Schrijver et al. 1989; Brandt & Solanki 1990; Zayer et al. 1990; Keller et al. 1990; Solanki & Brigljevic 1992; Rabin 1992).

At small filling factor, the equivalent widths of the Li I and K I features are nearly identical; towards larger α, they share similar behavior. The closeness of the curves demonstrates that K I 769.9 nm provides an excellent yardstick for gauging Li I 670.8 nm line strength variations that should not be attributed to abundance effects. In addition, the figure shows that spots and plage cause opposite line strength variation. Comparable computations for Ca II 854.2 nm (not shown) show slight decrease of W_λ with $\alpha_{\rm s}$, steep decrease with $\alpha_{\rm p}$.

Comparison with solar observations. The sunspot curve for K I 769.9 nm in Fig. 5 reaches equivalent width $W_\lambda \approx 0.12$ for unity filling factor, about six times enhancement over the RE value. This increase may be compared to the actual intensity equivalent width increase of the K I 769.9 nm line when observed from a solar umbra. The literature indicates K I umbral strengthening by only about a factor three (Bonet et al. 1988; Caccin et al. 1993; Severino et al. 1994) but inspection of the unpublished Kitt Peak FTS sunspot atlas used by the latter authors (prepared by N. Brynildsen, O. Engvold, V. Hansteen and J.W. Brault, and kindly forwarded to us by G. Severino) shows that this is an underestimate due to wing cutoffs at 90%. In our case, the full profile must be used for comparison with MULTI's results. Figure 6 shows a simple fit to the FTS scan which confirms that the line strengthens

to $W_\lambda > 0.1$ nm in umbra. The value for the quiet photosphere corresponds well with the 0.015 nm listed by Moore et al. (1966) which also underestimates the far wings.

The Li I 670.8 nm line strengthens from left to right in Fig. 5 by a factor of five. This is much smaller than the solar umbral strengthening by a factor forty reported by Giampapa (1984), but we regard the latter as an overestimation. A study being prepared by the Naples group, combining extensive observations of alkali resonance lines from solar active regions with elaborate line synthesis, shows that Li I 670.8 nm strengthens generally by a factor ten from quiet photosphere to umbrae (G. Cauzzi, private communication). The rest of the difference comes from the hundredfold larger lithium abundance which we employ here. At $A_{\rm Li} = 3.0$ the line saturates already in the nonmagnetic photosphere (Fig. 9 of Carlsson et al. 1994) and is very saturated in umbral spectra. Note that its magnetic splitting may be neglected at such high saturation, as we do here.

Comparison with stellar observations. Figure 7 compares our solar-model results with the data of Soderblom et al. (1993a) for solar-type stars in an observational format. The crosses represent an enlargement of the lefthand part of Fig. 1, without symbol coding. The abscissa again measures unreddened color B–V, i.e., with the corrections for interstellar reddening towards the Pleiades that were determined by Soderblom et al. (1993b) taken into account as specified in Table 1 of Soderblom et al. (1993a). This is the correct quantity to compare with our modeling which does not include interstellar reddening.

The Sun symbol is our result for the solar RE model. It represents an activity-free Pleiad that equals the quiet Sun in every respect except its lithium abundance. The dots are the results for adding sunspot umbrae and plage fluxtubes to it with filling factors $\alpha_{\rm s} = 0, \ldots, 0.5$ and $\alpha_{\rm p} = 0, \ldots, 0.5$. The dots fill a lozenge-shaped area (easiest noted in Fig. 11). Stars to which only spots are added make up the upper-left lozenge side, stars with pure plage the lower-left side.

This figure is the key plot of this paper. It shows that solar-like activity does not simply produce upward spread, as initially suspected from Fig. 1, but rather variations which are roughly aligned with the average trend of the $W_\lambda - (B$–$V)$ relation for G dwarfs. The reason is that both sunspots and solar plage fluxtubes produce appreciable reddening in comparison with the RE prediction. For sunspots the reddening is an expected color change, in keeping with the much lower effective temperature of the sunspot model in Fig. 2, but for plage the reddening is a surprise. It is due to the shallow plage temperature gradient around $h = 0$ (Fig. 2), and even exceeds the reddening by spots at equal filling factor.

The dots in Fig. 7 cover just about the observed spread in the G-star range ($0.58 < B$–$V < 0.80$) for both Li I 670.8 nm and K I 769.9 nm. However, they do so at large filling factors. The uppermost dot represents a solar-type star covered half by spot umbrae without plage, the lowest dot a star covered half by facular fluxtubes without umbrae. In actual solar active regions, the surface area occupied by umbrae tends to roughly equal the area occupied by facular fluxtubes (e.g., Schrijver 1987, Brandt & Solanki 1990, Steinegger et al. 1996).

If active Pleiades follow this solar balancing, their activity variations follow the long diagonal of the lozenge shape covered by the dots in Fig. 7. The maximum solar values of $\alpha_{\rm s}$ and $\alpha_{\rm p}$ are no larger than about 0.3% at the peak of the solar cycle (cf. Steinegger et al. 1996), so that the 50% umbra and 50% fluxtube coverage of the rightmost dot, leaving no space for any embedding quiet RE atmosphere, seems an unrealistic extrapolation of the solar paradigm. Even when that is taken for granted, it is hard to explain the K I 769.9 nm scatter from solar-like activity alone without invoking plage-covered stars without spots and vice versa.

In the G-star range both the observed spread (crosses) and the computed range covered by the dots are similar for the two lines, with the vertical extent of both variations a bit larger for K I 769.9 nm. This proves the point that the K I 769.9 nm spread must be explained before the Li I 670.8 nm spread is attributed to star-to-star abundance variations. In this part of the $W_\lambda - (B$–$V)$ diagram the observed spread of Li I 670.8 nm is relatively small (Fig. 1), but it does exceed the Hyades spread. In addition, the apparent correlations between line strength and chromospheric emission are most significant in this part of the diagram for both lines, indicating that the spread is not simply due to measurement scatter.

3.2. Stellar modeling

Figure 8 is the analog of Fig. 7 for our stellar modeling. The lefthand part of the figure contains modeling results for starspots with $T_{\rm eff} = 0.65\,T^*_{\rm eff}$ as well as for starspots with $T_{\rm eff} = 0.85\,T^*_{\rm eff}$. The latter produce smaller W_λ increase. The righthand part contains dots only for starspots with $T_{\rm eff} = 0.85\,T^*_{\rm eff}$ because there are no sufficiently cool models in the Uppsala grid for larger decrease (nor at 85% reduction for B–$V > 1.1$).

The effects of starspots and stellar plage, as represented by our models, are most easily separated for the RE model with B–$V = 1.04$ (rightmost diamond symbol). It sits at the lower-right corner of a lozenge covered by dots that describe the combination of spot effects (dotted side to the right and up for spots alone) and plage effects (dotted side to the left and down for plage only). Each RE model (diamond) has its attendant dot pattern.

The effect of plage is opposite to what is seen in Fig. 7. Our stellar plage modeling produces temperature stratifications that are both hotter and bluer than the corresponding RE atmosphere. They have no flat-gradient hump as in the solar plage model. As a result, all dots lie

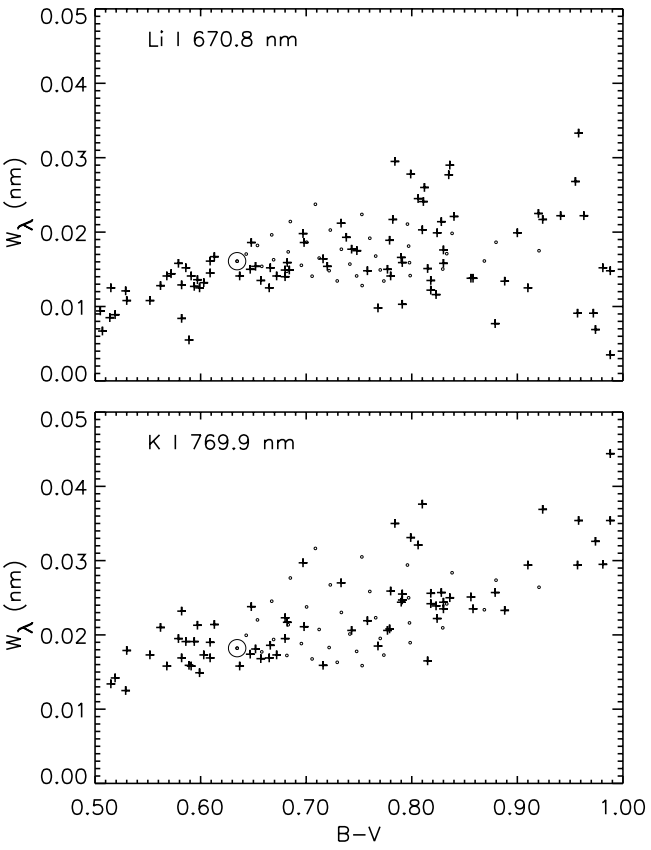

Fig. 7. Computed and observed equivalent widths of Li I 670.8 nm (*upper panel*) and K I 769.9 nm (*lower panel*) against color B–V, for the solar models. *Sun symbol:* line strength computed from the $T_{\rm eff} = 5750$ RE model. *Dots:* line strengths computed from mixtures of solar RE, sunspot and solar plage models. The spot and plage filling factors $\alpha_{\rm s}$ and $\alpha_{\rm p}$ vary each as $\alpha = 0, 0.1, \ldots, 0.5$. The dots mark all combinations, with the rightmost dot giving the result for a solar-type (but rather non-solar-like!) star that is covered half by sunspot umbrae and half by facular fluxtubes. Sunspots cause reddening plus increase of Li I and K I equivalent width. Solar plage causes yet larger reddening plus slight decrease of Li I and K I equivalent width. *Crosses:* observations by Soderblom et al. (1993a), the same as in Fig. 1

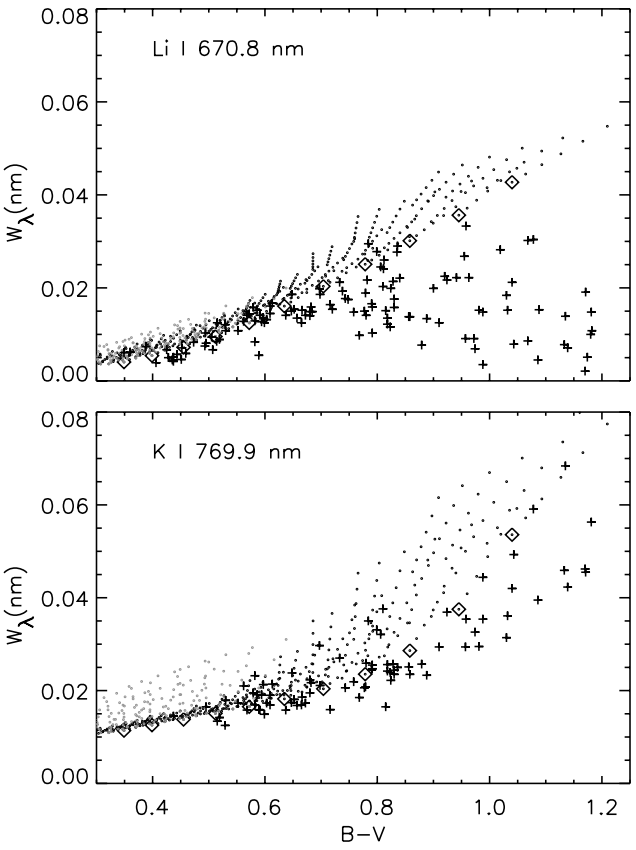

Fig. 8. Computed and observed equivalent widths of Li I 670.8 nm (*upper panel*) and K I 769.9 nm (*lower panel*) against color B–V, as in Fig. 7 but for the stellar modeling. *Diamond symbols:* line strength computed from the RE atmospheres. *Dots:* line strengths computed from mixtures of the RE atmospheres with starspots and stellar plage modeled by the simple recipes described in Sect. 2. The spot and plage filling factors $\alpha_{\rm s}$ and $\alpha_{\rm p}$ again vary each as $\alpha = 0, 0.1, \ldots, 0.5$. Starspots cause reddening plus line strength increase similarly to the sunspots in Fig. 7, but the stellar plage models produce opposite behavior by combining slight line strength decrease with appreciable decrease of B–V. *Crosses:* observations by Soderblom et al. (1993a), the same as in Fig. 1

on or above and to the left of the curve connecting the RE diamond symbols. This curve cuts through the middle of the scatter in the left half of the diagram, but even for K I 769.9 nm it lies well above most of the observed values in the right half of the diagram. Thus, even at unrealistically large filling factors our stellar activity modeling cannot explain the observed K I 769.9 nm spread. The same holds, a fortiori, for the Li I 670.8 nm spread in the upper panel.

4. Discussion

Computed spread versus observed spread. The G-star spread computed from the solar models more or less covers the observed spread for both Li I 670.8 nm and K I 769.9 nm (Fig. 7), but only when large filling factors, up to 50%, occur for spots and plage separately as well as in combinations.

For about equal contributions by these structures, as is roughly the case in solar active regions, the main effect of magnetic activity is to redden the star considerably. For both alkalis the long axis of the dotted lozenge in Fig. 7 lies along the average trend, with slight increase of W_λ along the axis for K I 769.9 nm and none for Li I 670.8 nm. The lozenge shape suggests that horizontal B–V shifts are rather more important in contributing to the observed spread in Fig. 1 than variation in W_λ. The computed $(\alpha_{\rm s} = 0.5, \alpha_{\rm p} = 0.5)$ shift of nearly 0.3 mag considerably

exceeds the overall Pleiades reddening of 0.04 mag derived by Soderblom et al. (1993b), apart from the eight exceptions in their Table 9, and it also exceeds the 0.05 mag reddening correction that Stauffer et al. (1984) found appropriate for ultrafast Pleiades rotators (cf. Soderblom 1989). The comparable results for our simplistic modeling of spots and plage on other stars (Fig. 8) differ markedly with respect to the effect of plage. In contrast to the solar fluxtubes, the stellar plage modeling decreases rather than increases B–V, so that the lozenge shapes point the other way. In addition, the RE models (diamond symbols) delineate the upper boundary of the observed spread for the cooler stars, not only for Li I 670.8 nm but also for the undepleted case of K I 769.9 nm. The excess indicates that either the RE models overestimate alkali line strengths considerably in the cooler part of Fig. 8, or/and that solar-like plage is prominent in all of these stars and causes large apparent reddening.

RE modeling versus line haze The RE models perform fairly well in the left half of Fig. 8 but seem to fail in the right half by producing excess K I 769.9 nm line strengths. Similar excess predictions are seen in comparable Na I D modeling for M giants of Tripicchio et al. (1996). They suggest that this deficiency is due to inadequate modeling of the ultraviolet line haze. The multitude of ultraviolet lines was taken into account LTE-wise in computing the Uppsala models, but not in our alkali line formation modeling. Its presence should diminish the actual photoionization rates from our computed values, causing larger neutral-stage fractions and equivalent widths than computed here. Such increase is indeed reported for the Na I D lines from M dwarfs by Andretta et al. (1996) when ultraviolet line opacities are added to MULTI's standard continuum opacities. However, our results above imply that this issue is not independent of the activity issue since our solar-like plage causes apparent reddening and our stellar plage recipe dereddens the star. Thus, apparently vertical equivalent width deficiencies may also portray horizontal color displacements in our graphs.

RE modeling versus granulation Convective energy transport is taken into account in the Uppsala MARCS code but the non-plane-parallel and dynamical effects of granulation are ignored in our line synthesis — except for the ubiquitous microturbulence parameter — and in our color evaluations. To what extent may granulation upset the computations? Our earlier study of alkali line formation from a detailed solar granulation simulation (Bruls & Rutten 1992) has shown that the solar Na I and K I resonance line profiles are quite sensitive to granular structuring. However, this sensitivity seems not to affect abundance determination very much. These lines are fairly well fitted with the meteoritic Na and K abundance values of Anders & Grevesse (1989), both when the turbulent and damping enhancement fudge parameters used in classical abundance determination are replaced by detailed NLTE and convectively structured line formation (Bruls & Rutten 1992) and when plane-parallel NLTE modeling is used without granulation but including classical turbulence and damping enhancements (Caccin et al. 1980, Severino et al. 1986). The same conclusion was reached directly from observations for a much larger line selection by Kiselman (1994). He used solar spectra with very high spatial resolution to measure spatial variations in equivalent widths and other parameters, and found that most lines do not possess the nonlinear variations that are required to upset spatially-averaged modeling. He so confirmed the point made by Holweger et al. (1990) that temperature gradients rather than the temperatures themselves or their influence on excitation and ionization set observed line strengths.

In utter contrast, Kurucz (1995) argues (in order to prove controversial ideas on cosmology presented in Kurucz 1992) that radiative overionization of lithium within the cool intergranular lanes of Population II stars leads to large underestimation of their actual lithium content when determined through classical plane-parallel abundance fitting (e.g., Molaro et al. 1995). Kurucz claims that this underestimation amounts to a full order of magnitude. However, his claim is qualitative, without detailed evaluation of the radiation fields that should ionize Li I in the intergranular lanes, and seems in conflict with the previous solar alkali results, with Kiselman's (1994) measurements, with the fact that Li I line strength is reduced by only a factor ten in much cooler umbrae, and with the older but still pertinent Fe I (another non-dominant ionization stage) analysis of Nordlund (1984). A detailed lithium-versus-granulation formation study is required to verify Kurucz' claim (Kiselman, in preparation). An obvious problem in this context is that the properties of non-solar stellar granulation are badly known except for the four case studies of Nordlund & Dravins (1990).

We should note here that the Pleiades spread discussed here is differential between similar stars. Even if the RE line haze and convection modeling is inadequate, similar stars should display similar granulation and suffer similar blanketing unless they differ in activity.

RE modeling versus abnormal granulation. Dan Kiselman (Stockholm) has pointed out to us that our modeling neglects "abnormal" granulation in plages. On the solar surface, plage is characterized by non-regular granulation in which large granules tend to be absent while small granular "fragments" abound. A vivid display of the difference with normal granulation is given by Fig. 6 (Plate 12) of Title et al. (1992), while comparison of plots B8 with plots C1 of Kiselman (1994) demonstrates appreciable difference in Fe I equivalent width behavior between normal and abnormal granulation.

If granulation affects lithium line strength sensitively, then the effect of the 100% surface filling factor of abnormal granulation within plage may actually outweigh the effect of the magnetic fluxtubes themselves.

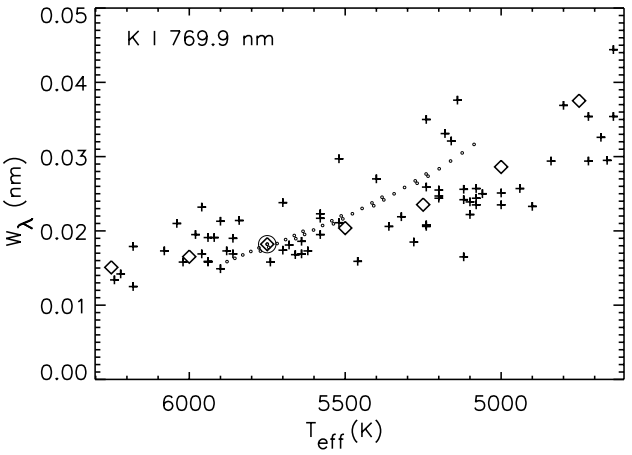

Fig. 9. Computed and observed equivalent widths of K I 769.9 nm as in Fig. 7, but plotted against effective temperature $T_{\rm eff}$ rather then color B–V. The crosses mark the observations of Soderblom et al. (1993a) at the $T_{\rm eff}$ values tabulated in their paper. The latter are based on standard B–V to $T_{\rm eff}$ conversion, whereas we have evaluated $T_{\rm eff}$ explicitly per atmospheric model combination (dots). The sunspot and solar plage fluxtube filling factors $\alpha_{\rm s}$ and $\alpha_{\rm p}$ again vary each as $\alpha = 0, 0.1, \ldots, 0.5$, but all dots happen to fall on a single curve which is rather close to the locus of the RE predictions (diamonds)

Color versus effective temperature. As noted in Sect. 2 we have explicitly evaluated both B–V and $T_{\rm eff}$ for each model mix. Figure 9 plots the computed K I 769.9 nm equivalent widths against the computed $T_{\rm eff}$ of the solar model combinations. The pattern made by the dots differs drastically from the lozenge shape in Fig. 7. The mixing of the different atmospheres produces effective temperature $T_{\rm eff} = [(1-\alpha_{\rm s}-\alpha_{\rm p})T_{\rm RE}^4 + \alpha_{\rm s}T_{\rm s}^4 + \alpha_{\rm p}T_{\rm p}^4]^{1/4}$ and this weighting happens to combine with the properties of the solar models such that all filling factor combinations produce dots along a narrow curve in the $W_\lambda - T_{\rm eff}$ diagram. It lies rather close to the locus of the RE models (diamonds). The large difference with the lozenge pattern in the lower panel of Fig. 7 shows that standard B–V to $T_{\rm eff}$ conversion is not valid for mixed atmospheres as the ones modeled here.

The crosses in Fig. 9 simply regain the pattern of the crosses in the lower panel of Fig. 7 because Soderblom et al. (1993a) used the standard B–V to $T_{\rm eff}$ conversion applied by Soderblom et al. (1993b). The large disparity between the dot patterns in the two figures demonstrates that observed and computed B–V is the quantity to use here.

Color versus color. In their Sect. 3.3, Soderblom et al. (1993a) use a two-color plot to argue against spots as a cause for the Pleiades Li I spread. At the suggestion of the referee, we emulate their Fig. 8 in our Fig. 10 by evaluating the Kron $(V{-}I)_K$ color for all our model mixes, again by direct numerical integration. The passbands of the Kron system (Kron & Smith 1951) were taken from http://obswww.unige.ch/gcpd/gcpd.html. We plot de-reddened B–V against uncorrected $(V{-}I)_K$ which makes the deviating Pleiades in Table 9 of Soderblom et al. (1993b) stand out, but does not affect the spread of the other stars. The band that the latter occupy is not narrower than the computed bands, both for the solar empirical modeling (top panel) and the stellar modeling (bottom panel). The sign of the effect of the plage contribution again flips between the two. The middle panel displays only the solar representatives of the stellar models in order to show the dependencies on the plage and spot filling factors more clearly. The conclusion is that the large color changes that activity causes in our modeling are not easily diagnosed from such two-color plots because the color changes follow the overall trend.

Diagnostic value of Li I 610.4 nm. A final test concerns the Li I 610.4 nm subordinate transition. Addition of this line as extra diagnostic to Li I 670.8 nm was recommended by Carlsson et al. (1994) because the NLTE formation properties of the two lines differ, with opposite LTE-to-NLTE correction at high lithium abundance. Similarly, Soderblom et al. (1993a) used the Li I 610.4 nm line to exclude chromospheric emission as a source of Li I 670.8 nm scatter. Their argument was, mistakenly, that the subordinate line is too weak to feel a chromosphere but is observed to vary along with the resonance line. As we have noted above, not even K I 769.9 nm feels the chromospheric temperature rise of our sunspot model, notwithstanding its large opacity, because NLTE resonance scattering fully uncouples the source function from the Planck function (Fig. 4). In fact, even the much stronger solar Na I D lines do not respond to the chromospheric temperature rise (Bruls et al. 1992), not even in sunspot umbrae (Severino et al. 1994). It takes stars with a much deeper-located chromospheric onset than the solar case to let Li I lines be affected directly by chromospheres (as opposed to being correlated with chromospheric emission as tell-tale of overall magnetic activity).

The erroneous suggestion that the two Li I lines should differ in chromospheric sensitivity was taken up recently by Russell (1996). He compares them for seven Pleiades and finds that the subordinate line produces higher lithium abundance, at smaller spread, than the resonance feature. The sample is too small for firm conclusions,

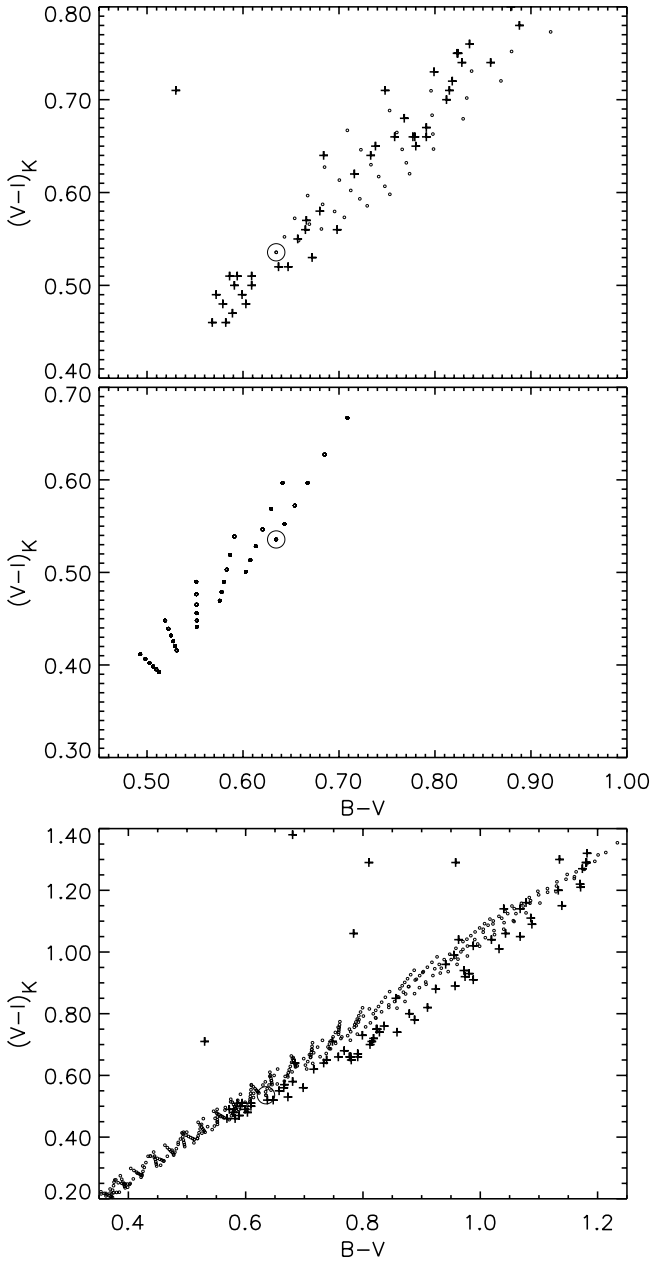

Fig. 10. Computed and observed color-color diagrams. Horizontal: dereddened B–V. The correction for interstellar reddening applied by Soderblom et al. (1993b) was $\Delta(B\text{–}V) = 0.04$ except for eight stars with $\Delta(B\text{–}V) > 0.2$ (their Table 9) of which seven make up the outlying crosses in the top and bottom panels. Vertical: Kron color $(V\text{–}I)_K$, without correction for interstellar reddening. Upper panel: observed values (crosses) compared with the solar spot and plage modeling. Middle panel: stellar spot and plage modeling for the solar RE model only, in order to display the computed dependencies on spots (increase to upper right) and plage (decrease to lower left). Bottom panel: observed values (crosses) compared with the stellar spot and plage modeling.

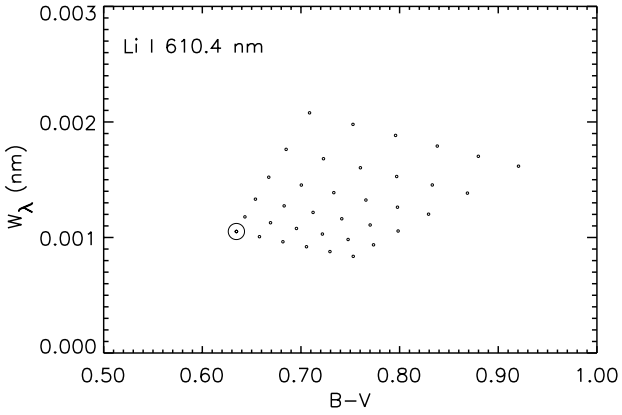

Fig. 11. Computed equivalent widths of the Li I 610.4 nm $3d$–$2p$ subordinate transition, for solar modeling as in Fig. 7

but indicates that studying Li I 610.4 nm along with Li I 670.8 nm for more Pleiades may be worthwhile — as suggested earlier by Duncan (1991).

However, diagnostic differences between Li I 610.4 nm and Li I 670.8 nm should not be large for the photospheric activity structures modeled here nor for the convective overionization invoked by Kurucz (1995). Spots, plage and convection affect primarily the photospheric stratification and the ionizing radiation fields, and thus affect primarily the photospheric ionization balances. To first order, these effects affect all alkali lines in similar fashion. This expectation is borne out by Fig. 11. It displays the results of our solar model grid for Li I 610.4 nm in the same format as Fig. 7. The horizontal extent of the lozenge-shaped pattern is the same as for Li I 610.4 nm and K I 769.9 nm, being set by the same reddening; the vertical extent of the pattern resembles that of Li I 670.8 nm, at ten times smaller but similar relative magnitude.

5. Conclusion

The bad coverage of the observed crosses by the computed dots in the upper panel of Fig. 8 might be taken as evidence that the Li I lines in the Pleiades do not suffer much from stellar activity, and so imply that Pleiades star-to-star Li I line strength variations may indeed be interpreted as due to intrinsic abundance variation. However, this conclusion is premature as long as the comparable K I 769.9 nm scatter in the lower panel of Fig. 8 is not satisfactorily reproduced. The K I 769.9 nm line turns out to be a valid proxy for estimating Li I 670.8 nm line strength variations that are not due to abundance variations (Fig. 5). The appreciable K I spread shown in Figs. 1 and 8 therefore remains an important warning flag. We so confirm the concluding statement of Carlsson et al. (1994).

Our results pose three more warnings. The first is that for increasing B–V the locus of the computed diamonds (RE models) and dots (mixed activity) in Fig. 8

departs from the observations. This excess signals a modeling deficiency that may be attributed to the ultraviolet line haze and/or to stellar surface convection. Neither is easily computed reliably. The second warning is that our solar and stellar plage models differ in sign in the changes they produce in both equivalent width and in broad-band color, Our solar plage model is a well-established empirical model while the stellar plage models are "best-effort" theoretical fluxtube ones. Their disparity in stratification (the hump shown in the upper panel of Fig, 2) causes large disparity between the corresponding results, signaling that simple constructs do not suffice for activity modeling. The third warning is that the broad-band color changes computed from our model mixes are large but are not easily diagnosed. In particular, care needs to be taken when converting B–V into $T_{\rm eff}$ at unknown color change (cf. Fuhrmann et al. 1994).

Neither our common-practice stellar activity modeling nor our more elaborate solar active-structure models succeed in reproducing the observed K I 769.9 nm scatter convincingly. The solar models do a better job than our stellar constructs, thanks to the reddening inherent in the solar plage stratification. However, even if we would take the solar modeling as correct, reproduction of the observed K I 769.9 nm spread for Pleiades G dwarfs requires the presence of stars that are excessively covered by spots without much plage as well as of stars that are excessively covered by plage without too many spots.

We conclude that the observed Pleiades K I 769.9 nm line strength variations are not easily explained by solar-like stellar activity, but that they do remain a matter of serious concern to discussions of Pleiades lithium abundance variations.

Acknowledgements. We thank Mats Carlsson for providing MULTI, the lithium model atom and the Uppsala model sequence. David Soderblom transmitted copies of viewgraphs used in his Florence Cool Star Workshop presentation. Steven Saar provided references to constrain the starspot models. Dan Kiselman suggested that abnormal granulation may affect the plage signal noticeably. The anonymous referee is thanked for his/her careful scrutiny and for suggesting various extensions to our study. Remko Stuik is indebted to the Studiefonds Kapteyn, the Olga Koningfonds and the Erasmus student exchange program for support, and gratefully thanks the Instituto de Astrofísica de Canarias for excellent hospitality.

References

Allen C. W. 1976, Astrophysical Quantities, Athlone Press, Univ. London

Anders E., Grevesse N. 1989, Geochim. Cosmochim. Acta, 53, 197

Andretta V., Byrne P. B., Doyle J. G. 1996, in R. Pallavicini, A. Dupree (eds.), Cool Stars, Stellar Systems, and the Sun, Procs. Ninth Cambridge Workshop, in press

Balachandran S., Lambert D. L., Stauffer J. R. 1988, ApJ, 333, 267

Bodenheimer P. 1965, ApJ, 142, 451

Boesgaard A. M. 1990a, in K. James (ed.), The formation and evolution of star clusters, Proc. 102nd Summer Meeting ASP, Astron. Soc. Pac. Conf. Series 13, p. 463

Boesgaard A. M. 1990b, in G. Wallerstein (ed.), Cool Stars, Stellar Systems and the Sun, Proc. Sixth Cambridge Workshop, Astron. Soc. Pac. Conf. Series 9, p. 317

Boesgaard A. M. 1991, ApJ, 370, L95

Bonet J. A., Marquez I., Vazquez M., Wöhl H. 1988, A&A, 198, 322

Bouvier J., Cabrit S., Fernández M., Martin E. L., Matthews J. M. 1993, A&A, 272, 176

Brandt P. N., Solanki S. K. 1990, A&A, 231, 221

Bruls J. H. M. J., Rutten R. J. 1992, A&A, 265, 257

Bruls J. H. M. J., Solanki S. K. 1993, A&A, 273, 293

Bruls J. H. M. J., Rutten R. J., Shchukina N. G. 1992, A&A, 265, 237

Bruning D. H. 1981, The applicability of the Fourier convolution theorem to the analysis of late-type stellar spectra, PhD Thesis New Mexico State Univ., Las Cruces

Butler R. P., Cohen R. D., Duncan D. K., Marcy G. W. 1987, ApJ, 319, L19

Byrne P. B. 1992, in P. Byrne, D. Mullan (eds.), Surface Inhomogeneities on Late-Type Stars, Springer, Berlin, p. 3

Caccin B., Gomez M. T., Roberti G. 1980, A&A, 92, 63

Caccin B., Gomez M. T., Severino G. 1993, A&A, 276, 219

Carlsson M. 1986, A Computer Program for Solving Multi-Level Non-LTE Radiative Transfer Problems in Moving or Static Atmospheres, Report No. 33, Uppsala Astronomical Observatory

Carlsson M., Rutten R. J., Bruls J. H. M. J., Shchukina N. G. 1994, A&A, 288, 860

Carlsson M., Rutten R. J., Shchukina N. G. 1992, A&A, 253, 567

Defouw R. J. 1976, ApJ, 209, 266

Duncan D. K. 1981, ApJ, 248, 651

Duncan D. K. 1991, ApJ, 373, 250

Duncan D. K., Jones B. F. 1983, ApJ, 271, 663

Favata F., Barbera M., Micela G., Sciortino S. 1995, A&A, 295, 147

Fuhrmann K., Axer M., Gehren T. 1994, A&A, 285, 585

Giampapa M. S. 1984, ApJ, 277, 235

Gray D. F. 1992, The Observation and Analysis of Stellar Photospheres, Cambridge Univ. Press, U.K. (second edition)

Greenstein J. L., Richardson R. S. 1951, ApJ, 113, 536

Gustafsson B., Bell R. A., Eriksson K., Nordlund Å.. 1975, A&A, 42, 407

Herbig G. H. 1965, ApJ, 141, 588

Holweger H., Heise C., Kock M. 1990, A&A, 232, 510

Hubeny I., Lanz T. 1995, ApJ, 439, 875

Hultqvist L. 1974, Solar Phys., 34, 25

Hultqvist L. 1977, Solar Phys., 52, 101

Iben I. V. 1965, ApJ, 142, 1447

Iben I. V. 1966, ApJ, 143, 483

Iben I. V. 1967, ApJ, 147, 624

Keller C. U., Solanki S. K., Steiner O., Stenflo J. O. 1990, A&A, 233, 583

Keller C. U., Stenflo J. O., Solanki S. K., Tarbell T. D., Title A. M. 1990, A&A, 236, 250

Kiselman D. 1994, Astronomy and Astrophysics Supplement Series, 104, 23

Kron G. E., Smith J. L. 1951, ApJ, 113, 324
Kurucz R. L. 1992, Comments Astrophys., 16, 1
Kurucz R. L. 1995, ApJ, 452, 102
Maltby P., Avrett E. H., Carlsson M. et al. 1986, ApJ, 306, 284
Michaud G., Charbonneau P. 1991, Space Sc. Rev., 57, 2
Molaro P., Primas F., Bonifacio P. 1995, A&A, 295, L47
Moore C. E., Minnaert M. G. J., Houtgast J. 1966, The Solar Spectrum 2935 Å to 8770 Å. Second Revision of Rowland's Preliminary Table of Solar Spectrum Wavelengths, NBS Monograph 61, National Bureau of Standards, Washington
Murphy R. J., Hua X.-M., Kozlovsky B., Ramaty R. 1990, ApJ, 351, 299
Neff J. E., O'Neal D., Saar S. H. 1995, ApJ, 452, 879
Nordlund Å. 1984, in S. L. Keil (ed.), Small-Scale Dynamical Processes in Quiet Stellar Atmospheres, National Solar Observatory Summer Conference, Sacramento Peak Observatory, Sunspot, p. 174
Nordlund A., Dravins D. 1990, A&A, 228, 155
O'Neil D., Saar S. H., Neff J. E. 1996, ApJ, 463, 766
Pallavicini R., Cerruti-Sola M., Duncan D. K. 1987, A&A, 174, 116
Pallavicini R., Randich S., Giampapa M. S. 1992, A&A, 253, 185
Pallavicini R., Cutisposo G., Randich S., Gratton R. 1993, A&A, 267, 145
Pinsonneault M. H., Kawaler S. D., Sofia S., Demarque P. 1989, ApJ, 338, 424
Pinsonneault M. H., Kawaler S. D., Demarque P. 1990, ApJS, 74, 501
Rabin D. 1992, ApJ, 391, 832
Randich S., Mark S G., Pallavicini R. 1992, in M. S. Giampapa, J. A. Bookbinder (eds.), Seventh Cambridge Workshop on Cool Stars, Stellar Systems and the Sun, Astron. Soc. Pac. Conf. Series, Vol. 26, p. 576
Randich S., Gratton R., Pallavicini R. 1993, A&A, 273, 194
Rebolo R. 1990, in F. Sanchez, M. Vazquez (eds.), New Windows to the Universe, Proc. XI ERAM IAU, Cambrige Univ. Press, Cambridge
Rebolo R. 1991, in G. Michaud, A. Tutukov (eds.), The Photospheric Abundance Connection, Proc. IAU Symp. 145, Kluwer, Dordrecht, p. 85
Robinson R. D., Thompson K., Innis J. L. 1986, Proc. Astron. Soc. Australia, 6, 4
Russell S. C. 1996, ApJ, 463, 593
Rutten R. J. 1996, Radiative Transfer in Stellar Atmospheres, Lecture Notes Utrecht University, 2nd WWW Edition
Rutten R. J., van der Zalm E. B. J. 1984, A&AS, 55, 171
Scharmer G. B., Carlsson M. 1985, J. Comput. Phys., 59, 56
Schrijver C. J. 1987, A&A, 180, 241
Schrijver C. J., Coté J., Zwaan C., Saar S. H. 1989, ApJ, 337, 964
Schüssler M. 1986, in W. Deinzer, M. Knölker, H. H. Voigt (eds.), Small Scale Magnetic Flux Concentrations in the Solar Photosphere, Abhandl. Akad. Wiss. Göttingen, Math.-Phys. Klasse Dritte Folge Nr. 38, Vandenhoeck und Ruprecht, Göttingen, p. 103
Severino G., Roberti G., Marmolino C., Gomez M. T. 1986, Solar Phys., 104, 259
Severino G., Gomez M. T., Caccin B. 1994, in R. J. Rutten, C. J. Schrijver (eds.), Solar Surface Magnetism, NATO ASI Series C 433, Kluwer, Dordrecht, p. 167
Soderblom D. R. 1989, ApJ, 342, 823
Soderblom D. R. 1991, in F. D'Antona (ed.), The Problem of Lithium, Proc. Workshop Monte Porzio, Mem. Soc. Astron. Ital., Vol. 62, No. 1, p. 43
Soderblom D. R. 1995, in F. Spite, R. Pallavicini (eds.), Stellar and interstellar lithium and primordial nucleosynthesis, Proc. IAU JD 11 The Hague, Mem. Soc. Astron. Ital., Vol 66, No 2, p. 347
Soderblom D. R. 1996, in R. Pallavicini, A. Dupree (eds.), Cool Stars, Stellar Systems, and the Sun, Procs. 9th Cambridge Workshop, ASP Conf. Series, in press
Soderblom D. R., Jones B. F., Balachandran S. et al. 1993a, AJ, 106, 1059
Soderblom D. R., Oey M. S., Johnson D. R. H., Stone R. P. S. 1990, AJ, 99, 595
Soderblom D. R., Stauffer J. R., Hudon J. D., Jones B. F. 1993b, ApJS, 85, 315
Soderblom D. R., Stauffer J. R., MacGregor K. B., Jones B. F. 1993c, ApJ, 409, 624
Solanki S. 1986, A&A, 168, 311
Solanki S. K., Brigljevic V. 1992, A&A, 262, L29
Spite F. 1990, in R. Pallavicini (ed.), High Resolution Spectroscopy in Astrophysics, Mem. Soc. Astron. Ital., Vol. 61, No. 3, p. 663
Spite F. 1991, in F. D'Antona (ed.), The Problem of Lithium, Proc. Workshop Monte Porzio, Mem. Soc. Astron. Ital., Vol. 62, No. 1, p. 11
Spite F. 1995, in F. Spite, R. Pallavicini (eds.), Stellar and interstellar lithium and primordial nucleosynthesis, Proc. IAU JD 11 The Hague, Mem. Soc. Astron. Ital., Vol 66, No 2, p. 517
Stauffer J. R., Hartmann L. W., Soderblom D. R., Burnham J. N. 1984, ApJ, 280, 202
Stauffer J. R., Prosser C. F., Giampapa M. S., Soderblom D. R., Simon T. 1993, AJ, 106, 229
Stauffer J. R., Caillault J.-P., Gagné M., Prosser C. F., Hartmann L. W. 1994, ApJS, 91, 625
Steinegger M., Vàzquez M., Bonet J. A., Brandt P. N. 1996, ApJ, 461, 478
Strom S. E. 1994, in J.-P. Caillault (ed.), Cool Stars, Stellar Systems, and the Sun, Procs. 8th Cambridge Workshop, ASP Conf. Series, 64, p. 211
Thorburn J. A. 1995, in F. Spite, R. Pallavicini (eds.), Stellar and interstellar lithium and primordial nucleosynthesis, Proc. IAU JD 11 The Hague, Mem. Soc. Astron. Ital., Vol 66, No 2, p. 313
Thorburn J. A., Hobbs L. M., Deliyannis C. P., Pinsonneault M. H. 1993, ApJ, 415, 150
Title A. M., Topka K. P., Tarbell T. D., Schmidt W., Balke C., Scharmer G. 1992, ApJ, 393, 782
Torres C. A. O., Mello S. F. 1973, A&A, 27, 231
Tripicchio A., Covino E., Gomez M. T., Severino G., Terranegra L. 1996, in R. Pallavicini, A. Dupree (eds.), Cool Stars, Stellar Systems, and the Sun, Proc. Ninth Cambridge Workshop, in press
Vogt S. S. 1981, ApJ, 250, 327
Wallerstein G., Herbig G. H., Conti P. S. 1965, ApJ, 141, 610
Wijbenga J. W., Zwaan C. 1972, Solar Phys., 23, 265

Zayer I., Stenflo J. O., Keller C. U., Solanki S. K. 1990, A&A, 239, 356

This article was processed by the author using Springer-Verlag LaTeX A&A style file *L-AA* version 3.